On the role of ice-nucleating aerosol in the formation of ice particles in tropical mesoscale convective systems

Ladino, Luis A.; Korolev, Alexei; Heckman, Ivan; Wolde, Mengistu; Fridlind, Ann M.; Ackerman, Andrew S.

Publisher's version / Version de l'éditeur:
https://doi.org/10.1002/2016GL072455
Geophysical Research Letters, 44, 3, pp. 1574-1582, 2017-02-04

AGU PUBLICATIONS

Geophysical Research Letters

RESEARCH LETTER
10.1002/2016GL072455

Key Points:
- Ice nuclei have minor contribution in the ice initiation in mesoscale convective systems
- Ice multiplication plays a dominant role in the cloud ice crystal formation in mesoscale convective systems
- Obtained new data on aerosol concentration near mesoscale convective systems

Supporting Information:
- Supporting Information SI

Correspondence to:
A. Korolev,
alexei.korolev@canada.ca

Citation:
Ladino, L. A., A. Korolev, I. Heckman, M. Wolde, A. M. Fridlind, and A. S. Ackerman (2017), On the role of ice-nucleating aerosol in the formation of ice particles in tropical mesoscale convective systems, *Geophys. Res. Lett.*, *44*, 1574–1582, doi:10.1002/2016GL072455.

Received 3 JAN 2017
Accepted 19 JAN 2017
Accepted article online 21 JAN 2017
Published online 4 FEB 2017

On the role of ice-nucleating aerosol in the formation of ice particles in tropical mesoscale convective systems

Luis A. Ladino[1,2], Alexei Korolev[1], Ivan Heckman[1], Mengistu Wolde[3], Ann M. Fridlind[4], and Andrew S. Ackerman[4]

[1]Cloud Physics and Severe Weather Research Section, Environment and Climate Change Canada, Toronto, Ontario, Canada, [2]Now at Centro de Ciencias de la Atmósfera, Universidad Nacional Autonoma de Mexico, México City, Mexico, [3]Flight Research Laboratory, National Research Council of Canada, Ottawa, Ontario, Canada, [4]NASA Goddard Institute for Space Studies, New York, New York, USA

Abstract Over the decades, the cloud physics community has debated the nature and role of aerosol particles in ice initiation. The present study shows that the measured concentration of ice crystals in tropical mesoscale convective systems exceeds the concentration of ice nucleating particles (INPs) by several orders of magnitude. The concentration of INPs was assessed from the measured aerosol particle concentration in the size range of 0.5 to 1 μm. The observations from this study suggest that primary ice crystals formed on INPs make only a minor contribution to the total concentration of ice crystals in tropical mesoscale convective systems. This is found by comparing the predicted INP number concentrations with in situ ice particle number concentrations. The obtained measurements suggest that ice multiplication is the likely explanation for the observed high concentrations of ice crystals in this type of convective system.

1. Introduction

The formation of ice in clouds is a key process that affects cloud lifetime [e.g., *Lohmann and Feichter*, 2005; *Cantrell and Heymsfield*, 2005], precipitation trends [e.g., *Lohmann and Feichter*, 2005; *Lawson et al.*, 2015], the Earth's radiative balance [e.g., *Lohmann and Feichter*, 2005; *Gayet et al.*, 2012; *Zeng et al.*, 2009], and the atmospheric electrification [e.g., *Williams et al.*, 1991], among other factors. At temperatures below −35°C, primary ice may effectively form via homogeneous nucleation of supercooled droplets or heterogeneous nucleation on ice nucleating particles (INPs) [e.g. *Rosenfeld and Woodley*, 2000; *Koop et al.*, 2000; *Möhler et al.*, 2003]. However, at warmer temperatures heterogeneous nucleation is considered to be a dominating mechanism of primary ice formation [e.g., *Vali*, 1985]. Therefore, it is expected that if ambient INPs are the only source of ice crystals, then the number concentrations of INPs should match or exceed [cf. *Fridlind et al.*, 2012] those of ice crystals within experimental uncertainties. However, numerous past and recent in situ observations reported that the measured number concentration of ice particles is actually much greater than the concentration of INPs, especially at high subzero temperatures (0°C > T > −15°C) [e.g., *Cooper and Vali*, 1981; *Field et al.*, 2001; *Baker and Lawson*, 2006; *Pratt et al.*, 2009; *Crawford et al.*, 2012; *Lloyd et al.*, 2015]. The early measurements are recognized as subject to contamination by shattered artifacts, which can result in an overestimation of the ice particles number concentration by up to 2 orders of magnitude [*Korolev et al.*, 2011; *Korolev et al.*, 2013a, 2013b]. These measurement artifacts provided a basis for arguing about incompleteness of evidence to conclude whether the concentrations of ice crystals and INPs are inconsistent with theoretical expectations. However, after applying new techniques to mitigate the effect of shattering on ice particle measurements [*Field et al.*, 2006; *Korolev et al.*, 2011; *Korolev et al.*, 2013a, 2013b; *Korolev and Field*, 2015], it was established here that the problem of ice crystal concentration exceeding that of INPs still persists. Explanation for the consistent difference between INP and ice particle concentrations highlighted in earlier studies [e.g., *Koenig*, 1963; *Mossop*, 1968, 1985; *Cantrell and Heymsfield*, 2005] still remains one of the long-standing problems in cloud physics.

Although it is widely recognized that the atmospheric aerosol plays important roles in cloud and precipitation microphysics [e.g., *Khain et al.*, 2005; *Li et al.*, 2011; *Fan et al.*, 2013; *Rosenfeld et al.*, 2014; *Chakraborty et al.*, 2016; *Seinfeld et al.*, 2016, and references therein], the understanding of their effect on the formation of ice is far from complete, both from theoretical and observational viewpoints [e.g., *DeMott et al.*, 2011;

Gayet et al., 2012; *DeMott et al*., 2016]. The link between aerosol concentration and the formation of ice crystals has been addressed through in situ measurements of INP concentrations [*DeMott et al*., 2010, and references therein] and by the sampling and subsequent analysis of ice crystal residuals [e.g., *Noone et al*., 1988; *Twohy and Poellot*, 2005; *Mertes et al*., 2007; *Pratt et al*., 2009; *Cziczo et al*., 2013; *Kupiszewski et al*., 2015]. Because of the complexity of airborne deployment and operation of existing INP counters, the scope of INP measurements in and nearby ice clouds remains limited. Such a limit to the measurements has hindered understanding of the INP role in ice formation.

The description of ice formation in cloud and climate models is linked to environmental parameters and aerosol properties [e.g., *Liu and Penner*, 2005; *Lohmann et al*., 2007; *Chen et al*., 2008; *Phillips et al*., 2008; *Hoose et al*., 2010; *Fridlind et al*., 2015; *Lloyd et al*., 2015; *Tan and Storelvmo*, 2016; *Twohy et al*., 2016]. In many numerical models ice initiation is based on parameterizations obtained from in situ observations of INPs [*Cooper*, 1986; *Meyers et al*., 1992; *DeMott et al*., 2010]. For example, the *DeMott et al*. [2010] parameterization (hereafter D10) predicts INP concentrations from the temperature and concentration of aerosol particles larger than 500 nm in diameter. Although the aforementioned parameterizations were developed based on INP measurements in a large variety of locations, once incorporated into numerical models, they are commonly insufficient for predicting ice particle concentrations and their size distributions [e.g., *Phillips et al*., 2003; *Fridlind et al*., 2007; *Joos et al*., 2008; *Klein et al*., 2009; *Morrison et al*., 2009; *Fridlind et al*., 2012; *Varble et al*., 2015; *Ackerman et al*., 2015; *Farrington et al*., 2016].

Secondary ice production has been suggested as one of the possible explanations of the discrepancy between the observed INPs and ice crystal concentrations. However, despite copious indirect evidence of ice multiplication [e.g., *Findeisen and Findeisen*, 1943; *Brewer and Palmer*, 1949; *Hallett and Mossop*, 1974; *Mossop*, 1985; *Beard*, 1992; *Heymsfield and Willis*, 2014; *Lawson et al*., 2015; *Ackerman et al*., 2015; *Taylor et al*., 2016, and references therein], until now, there is no direct confirmation of these processes, and the role of ice multiplication in ice initiation is still poorly understood. As reviewed by *Field et al*. [2016], there are several possible mechanisms by which secondary ice crystals can be formed. The best characterized and perhaps most efficient secondary ice production pathway is the so-called "rime splintering" or the "Hallett-Mossop (H-M) mechanism" [*Hallett and Mossop*, 1974]. Following the H-M mechanism formation of secondary ice crystals results from collisions of supercooled droplets and ice crystals (i.e., riming) at air temperatures ranging from −3 to −8°C with a maximum production rate at −5°C. Other mechanisms such as fracturing of drops or fracturing of ice crystals take place at lower temperatures than the H-M mechanism [e.g., *Bacon et al*., 1998, *Oraltay and Hallett*, 1989, *Vardiman*, 1978, *Field et al*., 2016, and others].

A number of recent studies have identified cloud regions with ice water content greater than 2 gm^{-3} and up to 6 g m^{-3} associated with high concentrations of ice crystals (up to 10^3 L^{-1}), a low concentration of graupel, and an absence of hail [*Lawson et al*., 1998; *Gayet et al*., 2012; *Fridlind et al*., 2015]. Concentrations of ice crystals exceeding 100 L^{-1} were also observed at temperatures as warm as −8°C in developing tropical cumulus [*Lawson et al*., 2015]. At present, the mechanisms underlying the formation of such high concentrations of ice crystals at subfreezing temperatures are not well understood. Given the importance of ice clouds in the hydrological cycle and radiation balance on global and regional scales, more research is needed to identify the mechanisms explaining the observed ice particle concentrations.

This study documents measurements of background aerosol particles at multiple altitudes in the vicinity of tropical mesoscale convective systems. It focuses on the analysis of the relationship between background aerosol and the concentration of ice crystals obtained from in situ measurements within the storms. The obtained results are relevant to the numerical simulation of such clouds in weather and climate models.

2. Methods

The data presented below were collected using the National Research Council (NRC) Convair 580 research aircraft during the High Altitude Ice Crystals—High Ice Water Content project [*Schwarzenboeck et al*., 2012; *Strapp et al*., 2016]. The flight operation was conducted out of Cayenne, French Guiana (4°56′14″N, 52°19′34″W) during rainy season in May 2015 (Figure S1 in the supporting information). Fourteen research flights were performed during this time. Environment and Climate Change Canada in collaboration with the NRC equipped the aircraft with a suite of in situ and remote sensing instruments for the characterization of aerosol and cloud microphysics and dynamics. Specifically, in this study, the analysis was focused on

Table 1. Summary of the Particle and Cloud Microphysics Probes Used for This Study

Name	Abbreviation	Purpose	Manufacturer	Nominal Size Range
Ultrahigh sensitivity aerosol spectrometer	UHSAS	Aerosol size and concentration	DMT	0.06–1 μm
Forward Scattering Spectrometer Probe	FSSP-100	Droplet size and concentration	PMS	2–32 μm or 2–47 μm
Optical Array Probe—2DC	OAP-2DC	Size and concentration of cloud ice crystals	PMS	50–1600 μm
2D-Stereo probe	2D-S	Size and concentration of cloud ice crystals	SPEC Inc.	10–1280 μm
Precipitation Imaging Probe	PIP	Size and concentration of precipitation particles	DMT	100–6400 μm

the measurements of the following instruments: (1) the ultrahigh sensitivity aerosol spectrometer (UHSAS) for measurements of the concentration and size distributions of aerosol particles [*Cai et al*., 2008]; (2) the Forward Scattering Spectrometer Probe (FSSP) [*Dye and Baumgardner*, 1984] for measurements of the concentration and size distribution of cloud droplets; and (3) the precipitation imaging probe (PIP) [*Baumgardner et al*., 2001], the two-dimensional stereo (2D-S) [*Lawson et al*., 2006], and the two-dimensional cloud (OAP-2DC) [*Knollenberg*, 1970] imaging probes for measurements of cloud and precipitation size particles. The nominal size ranges for each instrument are indicated in Table 1, and their mounting locations are shown in Figure 1. A brief description of the probes can be found in the supporting information. In order to mitigate the effect of shattering on the particle concentration measurements, the cloud particle probes were equipped with antishattering K-tips [*Korolev et al*., 2013b]. A modified interarrival time algorithm [*Field et al*., 2006; *Korolev and Field*, 2015] was applied to the imaging probes data to filter out the remaining shattering artifacts and minimize the effect of shattering on the calculated ice particle concentration. All probes were routinely checked and calibrated between the flight operations. This enabled the minimization of biases in measurements, providing reliable data sets.

During the flight operations the freezing level was typically located at 4800 m. Most sampling of ice crystals was conducted at altitudes in the range of 5700 to 7400 m, which corresponds to a temperature range from −5 to −15°C.

3. Results

3.1. Aerosol Vertical Profiles

In order to estimate the role of aerosol particles on cloud microstructure, the UHSAS concentration was integrated over the subrange from 500 nm to 1 μm and also over the full nominal range of this instrument down to 70 nm. For this specific data set the smaller UHSAS size bins were disregarded as they were suspect of contamination by electronic noise.

It was found that when flying through cloudy environments, the UHSAS aerosol concentration increased by 2 to 3 orders of magnitude compared to the measurements in clear sky (Figures S2 and S3). The effect of enhanced measured aerosol concentration in clouds has been previously documented in a number of studies [e.g., *Hudson and Frisbie*, 1991; *Weber et al*., 1998; and *Kleinman et al*., 2012]. The most likely explanation of such increase is that cloud particles shatter on impact with the UHSAS inlet, producing artificially high aerosol counts. Since there is no other physical mechanism explaining enhanced aerosol concentrations, the UHSAS measurements in clouds with total water content $TWC > 0.001\ g\ m^{-3}$ were identified as contaminated by artifacts, and they were excluded from the following analysis (see Figure S3).

The aerosol sampling was performed during ascent on transit to and descent on return from the region of cloud sampling in mesoscale convective systems (MCSs). The MCSs examined in the frame of this study had several hundred kilometers across and endurance no less than 8 h. These data were used to obtain the aerosol vertical profiles up to 6300 m on nine flights. Even though the aerosol sampling was horizontally extended over tens of kilometers, the vertical profiles of aerosol concentrations remained consistent within an order of magnitude on a flight-by-flight basis. Figure 2 shows the aerosol vertical profile averaged over the entire UHSAS data set. As expected, the aerosol concentration within the boundary layer (BL) was generally found to be greater than in the free troposphere with BL concentrations around $360\ cm^{-3}$ and $5.0\ cm^{-3}$ for particles ranging from 0.07 to 1 μm and 0.5 to 1 μm in diameter, respectively (see Figure S4 for more details). The

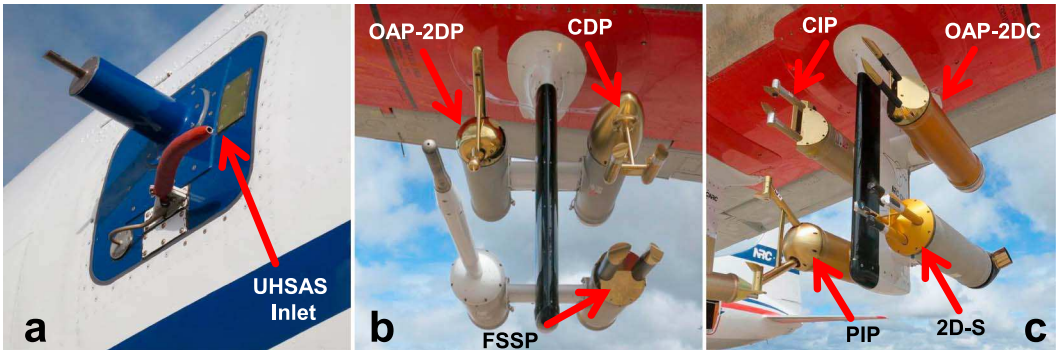

Figure 1. Mounting locations of the particle probes and the sampling inlets installed on the NRC Convair 580 (indicated by the red arrows). (a) UHSAS sampling inlet, (b) FSSP-100, and (c) the PIP, OAP-2DC and 2D-S probes.

measured aerosol concentration values are consistent with remote marine measurements obtained elsewhere at comparable particle size ranges using different instrumentation [e.g., *DeMott et al.*, 2003, and *Martin et al.*, 1994].

Analysis of the Hybrid Single-Particle Lagrangian Integrated Trajectory back trajectories [*Stein et al.*, 2015] (Figures S5 and S6) showed that the measured aerosol has a maritime origin, and it is presumably dominated by low-level sea-spray aerosol particles. This is consistent with the low values of the measured aerosol concentrations (Figure 2). The anthropogenic contribution into the aerosol concentration is considered as minor, since most of the flight operations were performed upwind of Cayenne.

A closer look at the aerosol size distributions at different altitudes is shown in Figure 3. The shape of the aerosol particle size distribution remained approximately constant with altitude. Compared with the stable bimodal aerosol size distributions found by *Krejci et al.* [2005] in the marine BL in the Cayenne region and during the same time of year, these size distributions appear to be representative of Aitken mode particles that either did not undergo significant cloud processing or were subject to precipitation scavenging of accumulation mode particles.

3.2. Aerosol Concentration Versus Ice Particle Number Concentration

The ice particle size distributions, concentrations, and ice water contents (IWCs) were calculated from the composite 2D-S and PIP data. The first three size bins in PSDs were ignored in estimations of the ice particle concentration owing to large ambiguity in sample area definition and increased susceptibility to different types of errors [*Korolev et al.*, 1998; *Korolev and Field*, 2015]. Thus, out-of-focus broken images (1–3 pixels) may significantly contribute to an artificial enhancement of the 2D-S concentration of small cloud particles. Omission of the first three 2D-S size bins results in reduction of the measured ice crystal concentration by approximately one half (Figures S7 and S8). This presents a conservative assessment of the ice crystal concentration, and it does not affect the main conclusion obtained in this study. The IWC calculated from the composite size distributions were typically below 2–3 $g\,m^{-3}$, peaking up to 4 $g\,m^{-3}$ in some cloud regions, with an estimated uncertainty of roughly less than 20%. These values are in good agreement with the simultaneous IWC bulk measurements from the Convair 580 and consistent with previous MCS studies by other research groups [*Gayet et al.*, 2012; *Fridlind et al.*, 2015; *Lawson et al.*, 2015]. The average ice particle concentration was found to be approximately 200 L^{-1} (ranging from $10^{-2}\,L^{-1}$ to $10^{3}\,L^{-1}$) at altitudes between 4800 and 7400 m as shown by the blue and black solid lines in Figure 4. Most of the ice crystals were found to be smaller than 700 μm in diameter (see Figure S9).

If all the measured ice crystals were formed on INPs and sedimentation divergence can be neglected, then the ice particle concentration should not exceed INP concentrations. In contrast, with the cloud condensation nuclei, INPs represent only a small fraction of the total aerosol particle population (1 in 10^6 or fewer). The concentration of INPs can be estimated from the D10 parameterization relating number concentrations of aerosol and INPs as a function of temperature, based on measurements at temperatures between −35 and −9°C:

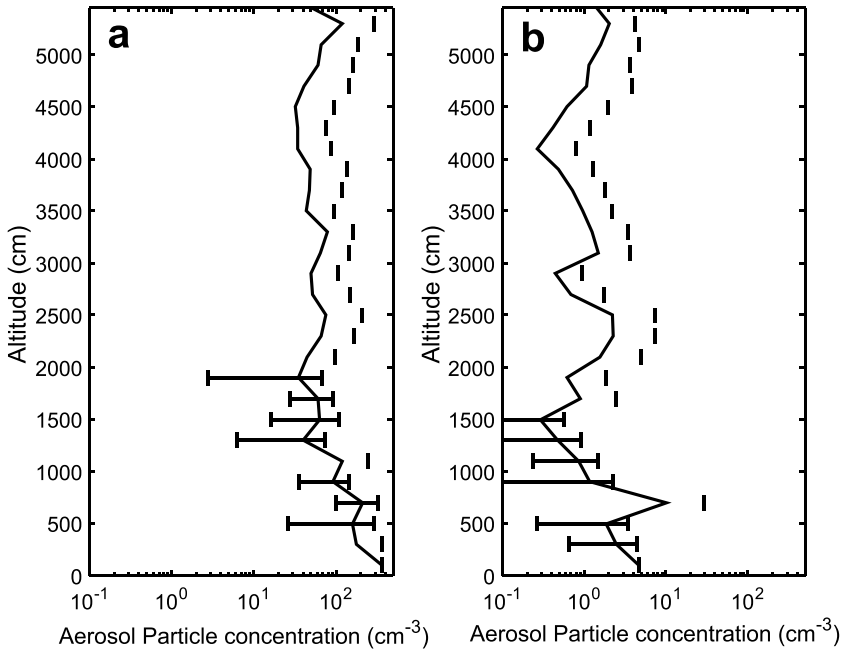

Figure 2. Vertical profiles of the average aerosol number concentration (every 200 m) measured with the UHSAS for size ranges (a) 70 nm $< D_p <$ 1 μm and (b) 500 nm $< D_p <$ 1 μm.

$$n_{\mathrm{INP},T_k} = a(273.16 - T_k)^b \left(n_{\mathrm{aer},0.5}\right)^{c(273.16-T_k)+d}, \quad (1)$$

where $n_{\mathrm{INP},Tk}$ is the predicted INP in standard L^{-1}, T_k is the temperature in Kelvin, $n_{\mathrm{aer},0.5}$ is the aerosol concentration for particles larger than 500 nm diameter in cm^{-3}, $a = 0.0000594$, $b = 3.33$, and $c = 0.0264$, and $d = 0.0033$ [*DeMott et al.*, 2010].

Figure 4 and Table S1 show the concentration of INPs calculated from equation (1) for $n_{\mathrm{aer},0.5}$ corresponding to the concentration of aerosol particles with diameter 0.5–1 μm as measured by the UHSAS at different altitude in the free troposphere and the boundary layer. Since D10 most commonly used 1–3 μm as upper limit, it is anticipated that equation (1) may underestimate the INP concentration, if $n_{\mathrm{aer},0.5}$ is truncated at 1 μm. The contribution of the aerosol concentration from 1–3 μm into the INP concentration was assessed based on linear extrapolation of the UHSAS aerosol size distribution towards large sizes. The obtained estimate suggests that, based on equation (1), the aerosol concentration from the size range 1–3 μm contributes to n_{INP,T_k} no more than 4% at -15°C. Such underestimation of the INP concentration in terms of the D10 formalism is quite small and does not affect the main outcomes of this study. However, for future similar studies it is recommended that measurements of aerosol size distributions span a size range of 0.5 ÷ 3 μm in diameter.

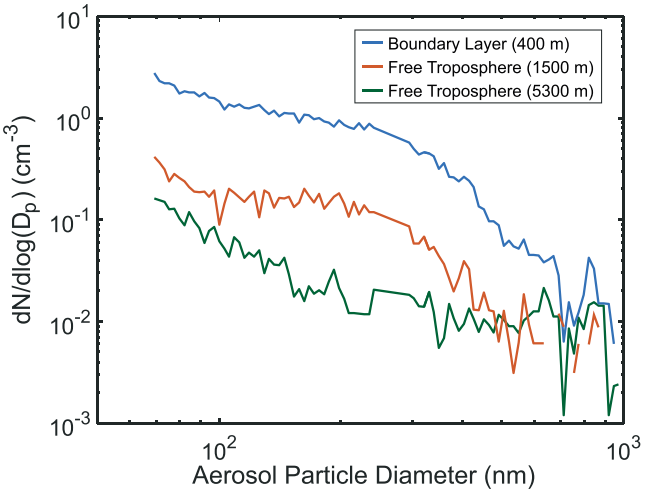

Figure 3. Example of the aerosol size distributions measured in the boundary layer (blue) and free troposphere (red and orange) measured UHSAS in the vicinity of MCSs in the Cayenne region.

As seen from Figure 4, the average concentration of ice crystals exceeds the estimated INP concentrations by up to 4 orders of magnitude at −5°C

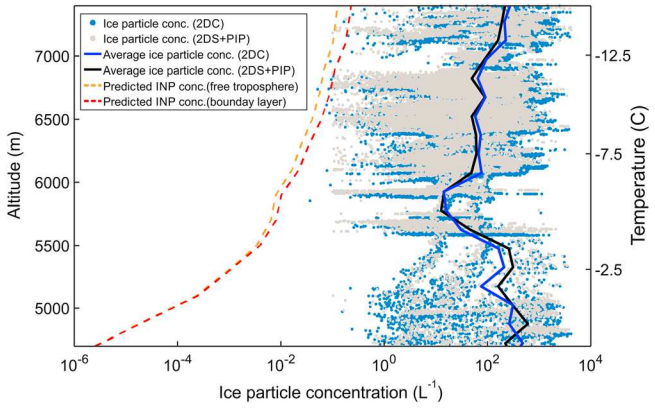

Figure 4. Comparisons of measured average concentrations of INP (dashed lines) and ice crystals (solid lines). INP concentration was calculated from the UHSAS aerosol measurements based on the *DeMott et al.* [2010] parameterization. The UHSAS concentration was measured in the vicinity of MCSs. Dots indicate 1 s average ice crystal concentrations measured inside MCSs by 2DC (blue) and 2D-S + PIP (grey). The concentrations from the 2D-S correspond to particles larger than 40 μm diameter.

and by 2 orders of magnitude at −14°C. This difference remains even if the maximum aerosol concentration from the boundary layer is used to predict the INP concentrations (red dashed line in Figure 4). The fluctuations shown by the dashed lines in Figure 4 are the result of averaging multiple temperature vertical profiles. At approximately −5°C, corresponding to the maximum productivity of the H-M mechanism, the predicted INP concentration in the present study (i.e., $6\times10^{-3}\,L^{-1}$) is higher but close to those recently reported by *Petters and Wright* [2015] (from 10^{-3} to $10^{-5}\,L^{-1}$), *DeMott et al.* [2016] ($2\times10^{-5}\,L^{-1}$, for maritime environments), and *Twohy et al.* [2016] ($10^{-3}\,L^{-1}$). Since for the altitude above 6300 m the UHSAS measurements were not available and for the altitude above 5700 m there is UHSAS data for one flight only, $n_{aer,0.5}$ in equation (1) was assumed constant and equal to $0.9\,cm^{-3}$ above 5700 m. This assumption is supported by a weak dependence of $n_{aer,0.5}$ at lower levels in the free troposphere (i.e., the average aerosol concentration for particle diameter $D_p > 500$ nm is $0.9\pm0.52\,cm^{-3}$ between 2900 m and 5700 m).

Based on the data shown in Figure 4, primary ice crystals formed through INPs cannot be the main contributors to total ice particle number concentrations. However, the presence of primary ice crystals may be important to trigger the formation of secondary ice crystals through different mechanisms. As reviewed by *Field et al.* [2016], the secondary ice production rate has been previously linked to the number density of primary ice crystals. For example, *Beard* [1992] found that a low concentration of primary ice crystals (i.e., 10^{-3}–$10^{-5}\,L^{-1}$) is sufficient to trigger ice multiplication. More recently, *Crawford et al.* [2012] found that an ice concentration of $100\,L^{-1}$ measured in shallow convective clouds over the southern UK can be explained by secondary ice crystals production triggered by the presence of a low concentration of INPs (on the order of $10^{-2}\,L^{-1}$) via the H-M mechanism.

Although the tropical MCSs and the shallow convective clouds are quite different in terms of dimensions, longevity, and dynamics, it is notable that ice particle concentrations and INP concentrations reported in the present study and in *Crawford et al.* [2012] are very similar. The observations made in the present study do not specifically pinpoint the H-M mechanism, as secondary ice crystals may also have formed via other mechanisms such as the fragmentation of drops during freezing [e.g., *Fridlind et al.*, 2007; *Ackerman et al.*, 2015; *Kiselev et al.*, 2016 and references therein]. In some cases, graupel formed at higher levels was observed at temperatures close to −5°C with conditions favorable for the H-M mechanism. However, in most cases graupel was not present, but ice crystals identified as potential secondary ice at high concentrations were still observed (see Figure S10).

4. Discussion and Conclusions

Vertical profiles (up to 7400 m) of the aerosol and ice crystal concentrations were obtained from in situ measurements in mesoscale convective systems out of Cayenne. These profiles were explored with the aim to estimate the role of background submicron aerosol particles in the formation of high ice concentration in MCSs. It was found that the average concentration of submicron aerosol in the free troposphere with $D_p > 500$ nm and $D_p > 70$ nm was approximately 0.9 and $60\,cm^{-3}$, respectively, and it remained rather stable for the entire days of the flight operations. In the boundary layer, the aerosol concentration varied between 0.8 and $5.0\,cm^{-3}$ for particles larger than 500 nm and between 150 and $360\,cm^{-3}$ for particles larger than 70 nm.

The aerosol concentrations measured by the UHSAS were used to predict the INP concentrations following the parameterization derived by *DeMott et al*. [2010]. It was found that the predicted INP concentration is orders of magnitudes lower than the concentration of ice crystals measured at the same levels. This result suggests that the measured concentrations of aerosol particles are not sufficient in explaining the formation of the observed concentration ice crystals through primary heterogeneous nucleation of INPs. The most likely explanation of the observed concentration of ice crystals is related to secondary ice production mechanisms such as the H-M mechanism or droplet fragmentation during freezing. Such a conclusion was also reached by *Ackerman et al*. [2015] from analysis focused on ice particle sizes instead of number concentrations. A deeper analysis, so as to identify the most important secondary ice formation mechanism, will be addressed in a follow-up study.

The formation of primary ice crystals at temperatures close to 0°C is only possible on efficient INPs such as biological particles or soil-dust organic-rich particles [*Hoose and Möhler*, 2012]; however, primary biological aerosol particle concentrations, and hence the INP concentrations at subzero temperatures, can be far too low to explain observed ice particle number concentrations [*Conen et al*., 2011; *Tobo et al*., 2013; *O'Sullivan et al*., 2014; *Wilson et al*., 2015; *DeMott et al*., 2016; *Petters and Wright*, 2015; *Twohy et al*., 2016]. For example, *Petters and Wright* [2015] and *DeMott et al*. [2016] reported that at −5°C, measured INP concentrations range from 10^{-3} to $10^{-6}\,L^{-1}$ for maritime environments. Therefore, the present results suggest that although submicron aerosol particles are not entirely responsible for the formation of the high concentration of ice crystals observed in convective cloud regions in MCSs, they can trigger the formation of secondary ice crystals through heterogeneous nucleation of primary ice crystals. Although our findings are in agreement with previous studies, the novel features of this study can be formulated as follows: (a) a statistically significant data set on aerosol size distribution in the vicinity of tropical MCSs was obtained; (b) the suite of cloud particle probes (7 in total Figures 1b and 1c) equipped with antishattering tips along with the use of advanced processing software enabled obtaining highly reliable and redundant measurements of ice particle concentration in MCSs, which are possible today; (c) the measurements in (a) and (b) were conducted on the same spatial and temporal scales, which has allowed us to draw a justifiable conclusion about secondary ice production in MCSs.

The present results should contribute to a better understanding of cloud processes in weather prediction and climate models.

Acknowledgments

ECCC participation in the HIWC program was supported by Transport Canada and the Federal Aviation Administration. The NRC RAIR program has generously provided partial funding for this project. The authors are grateful for the technical support provided during the data collection period and would like to thank Mohammed Wasey, Michel Harwood, Jason Iwachow (ECCC); Anne Marie McDonald (ECCC) for sharing the UHSAS; Gary Giles, Eric Roux, and Mathew Bastian (NRC); and the NRC Convair 580 Aircraft Maintenance Engineers. Special thanks to the NRC FRL pilots Paul Kissman, Anthony Brown, and Rob Erdos for their outstanding cooperation and aircraft navigation through convective cloud regions during the data collection. Authors appreciate Walter Strapp (MetAnalyics Inc.), Tom Ratvasky, and Kurt Blankenship (NASA GRC) for the ground support of the Convair 580 flight operations. L.A. Ladino thanks the Natural Sciences and Engineering Research Council of Canada (NSERC) for his fellowship. A.M. Fridlind and A.S. Ackerman thank the NASA Modeling and Analysis Program for funding their contribution to this study. The data used in this study are available at Environment and Climate Change Canada upon request from Alexei Korolev (alexei.korolev@canada.ca).

References

Ackerman, A. S., et al. (2015), High ice water content at low radar reflectivity near deep convection–Part 2: Evaluation of microphysical pathways in updraft parcel simulations, *Atmos. Chem. Phys.*, *15*(20), 11,729–11,751, doi:10.5194/acp-15-11729-2015.

Bacon, N. J., B. D. Swanson, M. Baker, and E. Davis (1998), Breakup of levitated frost particles, *J. Geophys. Res.*, *103*(D12), 13,763–13,775, doi:10.1029/98JD01162.

Baker, B. A., and R. P. Lawson (2006), In situ observations of the microphysical properties of wave, cirrus, and anvil clouds. Part I: Wave clouds, *J. Atmos. Sci.*, *63*, 3160–3185, doi:10.1175/JAS3802.1.

Baumgardner, D., H. Jonsson, W. Dawson, D. O'Connor, and R. Newton (2001), The cloud, aerosol and precipitation spectrometer: A new instrument for cloud investigations, *Atmos. Res.*, *59*, 251–264, doi:10.1016/S0169-8095(01)00119-3.

Beard, K. V. (1992), Ice initiation in warm-base convective clouds: An assessment of microphysical mechanisms, *Atmos. Res.*, *28*(2), 125–152.

Brewer, A. W., and H. P. Palmer (1949), Condensation processes at low temperatures, and the production of new sublimation nuclei by the splintering of ice, *Nature*, *164*, 312–313, doi:10.1038/164312a0.

Cai, Y., D. C. Montague, W. Mooiweer-Bryan, and T. Deshler (2008), Performance characteristics of the ultra high sensitivity aerosol spectrometer for particles between 55 and 800 nm: Laboratory and field studies, *J. Aerosol Sci.*, *39*, 759–769, doi:10.1016/j.jaerosci.2008.04.007.

Cantrell, W., and A. Heymsfield (2005), Production of ice in tropospheric clouds: A review, *Bull. Am. Meteorol. Soc.*, *86*, 795–807, doi:10.1175/BAMS-86-6-795.

Chakraborty, S., R. Fu, S. T. Massie, and G. Stephens (2016), Relative influence of meteorological conditions and aerosols on the lifetime of mesoscale convective systems, *Proc. Natl. Acad. Sci. U.S.A.*, 201601935, *113*(27), 7426–7431, doi:10.1073/pnas.1601935113.

Chen, J. P., A. Hazra, and Z. Levin (2008), Parameterizing ice nucleation rates using contact angle and activation energy derived from laboratory data, *Atmos. Chem. Phys.*, *8*, 7431–7449, doi:10.5194/acp-8-7431-2008.

Conen, F., S. Henne, C. Morris, and C. Alewell (2011), Atmospheric ice nucleators active ≥− 12 °C may be quantified on PM10 filters, *Atmos. Meas. Tech.*, *5*, 321–327, doi:10.5194/amt-5-321-2012.

Cooper, W. A. (1986), Ice initiation in natural clouds, *Meteor. Mon.*, *21*, 29–32, doi:10.1175/0065-9401-21.43.29.

Cooper, W. A., and G. Vali (1981), The origin of ice in mountain cap clouds, *J. Atmos. Sci.*, *38*, 1244–1259, doi:10.1175/1520-0469(1981)038<1244:TOOIIM>2.0.CO;2.

Crawford, I., et al. (2012), Ice formation and development in aged, wintertime cumulus over the UK: Observations and modelling, *Atmos. Chem. Phys.*, *12*, 4963–4985, doi:10.5194/acp-12-4963-2012.

Cziczo, D. J., et al. (2013), Clarifying the dominant sources and mechanisms of cirrus cloud formation, *Science*, *340*(6138), 1320–1324, doi:10.1126/science.1234145.

DeMott, P. J., et al. (2010), Predicting global atmospheric ice nuclei distributions and their impacts on climate, *Proc. Natl. Acad. Sci. U.S.A.*, *107*, 11,217–11,222, doi:10.1073/pnas.0910818107.
DeMott, P., K. Sassen, M. Poellot, D. Baumgardner, D. Rogers, S. Brooks, A. Prenni, and S. Kreidenweis (2003), African dust aerosols as atmospheric ice nuclei, *Geophys. Res. Lett.*, *30*, 1732, doi:10.1029/2003GL017410.
DeMott, P. J., et al. (2011), Resurgence in ice nuclei measurement research, *Bull. Am. Meteorol. Soc.*, *92*, 1623–1635, doi:10.1175/2011BAMS3119.1.
DeMott, P. J., et al. (2016), Sea spray aerosol as a unique source of ice nucleating particles, *Proc. Natl. Acad. Sci. U.S.A.*, *113*, 5797–5803, doi:10.1073/pnas.1514034112.
Dye, J. E., and D. Baumgardner (1984), Evaluation of the forward scattering spectrometer probe. Part I: Electronic and optical studies, *J. Atmos. Oceanic Tech.*, *1*(4), 329–344, doi:10.1175/1520-0426(1984)001<0329:EOTFSS>2.0.CO;2.
Fan, F., et al. (2013), Microphysical effects determine macrophysical response for aerosol impact on deep convective clouds, *Proc. Natl. Acad. Sci. U.S.A.*, *110*, E4581–E4590, doi:10.1073/pnas.1316830110.
Farrington, R. J., et al. (2016), Comparing model and measured ice crystal concentrations in orographic clouds during the INUPIAQ campaign, *Atmos. Chem. Phys.*, *16*, 4945–4966, doi:10.5194/acp-16-4945-2016.
Field, P. R., et al. (2001), Ice nucleation in orographic wave clouds: Measurements made during INTACC, *Q. J. R. Meteorol. Soc.*, *127*, 1493–1512, doi:10.1002/qj.49712757502.
Field, P. R., A. J. Heymsfield, and A. Bansemer (2006), Shattering and particle inter-arrival times measured by optical array probes in ice clouds, *J. Atmos. Oceanic Tech.*, *23*, 1357–1370, doi:10.1175/JTECH1922.1.
Field, P. R., et al. (2016), Ice formation and evolution in clouds and precipitation: Measurement and modeling challenges. Chapter 7: Secondary ice production-current state of the science and recommendations for the future, *Meteor. Monogr.*, 1–53, doi:10.1175/AMSMONOGRAPHS-D-16-0014.1, in press.
Findeisen, W., and E. Findeisen (1943), Investigations on the ice splinter formation on rime layers (a contribution to the origin of storm electricity and the microstructure of cumulonimbi), *Meteor. Z.*, *60*(5).
Fridlind, A. M., et al. (2007), Ice properties of single-layer stratocumulus during the Mixed-Phase Arctic Cloud Experiment: 2. Model results, *J. Geophys. Res.*, *112*, D24202, doi:10.1029/2007JD008646.
Fridlind, A. M., et al. (2012), A comparison of TWP-ICE observational data with cloud-resolving model results, *J. Geophys. Res.*, *117*, D05204, doi:10.1029/2011JD016595.
Fridlind, A. M., et al. (2015), High ice water content at low radar reflectivity near deep convection–Part 1: Consistency of in situ and remote-sensing observations with stratiform rain column simulations, *Atmos. Chem. Phys.*, *15*(20), 11,713–11,728, doi:10.5194/acp-15-11713-2015.
Gayet, J. F., et al. (2012), On the observation of unusual high concentration of small chain-like aggregate ice crystals and large ice water contents near the top of a deep convective cloud during the CIRCLE-2 experiment, *Atmos. Chem. Phys.*, *12*, 727–744, doi:10.5194/acp-12-727-2012.
Hallett, J., and S. C. Mossop (1974), Production of secondary ice particles during the riming process, *Nature*, *249*, 26–28, doi:10.1038/249026a0.
Heymsfield, A. J., and P. Willis (2014), Cloud conditions favoring secondary ice particle production in tropical maritime convection, *J. Atmos. Sci.*, *71*, 4500–4526, doi:10.1175/JAS-D-14-0093.1.
Hoose, C., and O. Möhler (2012), Heterogeneous ice nucleation on atmospheric aerosols: A review of results from laboratory experiments, *Atmos. Chem. Phys.*, *12*, 9817–9854, doi:10.5194/acp-12-9817-2012.
Hoose, C., J. E. Kristjánsson, J. P. Chen, and A. Hazra (2010), A classical-theory-based parameterization of heterogeneous ice nucleation by mineral dust, soot, and biological particles in a global climate model, *J. Atmos. Sci.*, *67*, 2483–2503, doi:10.1175/2010JAS3425.1.
Hudson, J. G., and P. R. Frisbie (1991), Cloud condensation nuclei near marine stratus, *J. Geophys. Res.*, *96*, 20,795–20,808, doi:10.1029/91JD02212.
Joos, H., P. Spichtinger, U. Lohmann, J. F. Gayet, and A. Minikin (2008), Orographic cirrus in the global climate model ECHAM5, *J. Geophys. Res.*, *113*, doi:10.1029/2007JD009605.
Khain, A., D. Rosenfeld, and A. Pokrovsky (2005), Aerosol impact on the dynamics and microphysics of deep convective clouds, *Q. J. R. Meteorol. Soc.*, *131*, 2639–2663, doi:10.1256/qj.04.62.
Kiselev, A., A. Lauber, P. Handmann, T. Pander, T. Leisner (2016), Production of secondary ice particles and splintering of freezing droplets as a potential mechanism of ice multiplication. ICCP, 25-29 July, 2016, Manchester, U. K.
Klein, S. A., et al. (2009), Intercomparison of model simulations of mixed-phase clouds observed during the ARM Mixed-Phase Arctic Cloud Experiment. I: Single-layer cloud, *Q. J. R. Meteorol. Soc.*, *135*, 979–1002, doi:10.1002/qj.416.
Kleinman, L. I., et al. (2012), Aerosol concentration and size distribution measured below, in, and above cloud from the DOE G-1 during VOCALS-REx, *Atmos. Chem. Phys.*, *12*, 207–223, doi:10.5194/acp-12-207-2012.
Knollenberg, R. G. (1970), The optical array: An alternative to scattering or extinction for airborne particle size determination, *J. Appl. Meteorol.*, *9*(1), 86–103, doi:10.1175/1520-0450(1970)009<0086:TOAAAT>2.0.CO;2.
Koenig, L. R. (1963), The glaciating behavior of small cumulonimbus clouds, *J. Atmos. Sci.*, *20*, 29–47, doi:10.1175/1520-0469(1963)020<0029:TGBOSC>2.0.CO;2.
Koop, T., B. P. Luo, A. Tsias, and T. Peter (2000), Water activity as the determinant for homogeneous ice nucleation in aqueous solutions, *Nature*, *406*, 611–614, doi:10.1038/35020537.
Korolev, A., and P. R. Field (2015), Assessment of the performance of the inter-arrival time algorithm to identify ice shattering artifacts in cloud particle probe measurements, *Atmos. Meas. Tech.*, *8*, 761–777, doi:10.5194/amt-8-761-2015.
Korolev, A. V., J. W. Strapp, and G. A. Isaac (1998), Evaluation of accuracy of PMS optical array probes, *J. Atmos. Oceanic Tech.*, *15*, 708–720, doi:10.1175/1520-0426(1998)015<0708:EOTAOP>2.0.CO;2.
Korolev, A., E. Emery, and K. Creelman (2013b), Modification and tests of particle probe tips to mitigate effects of ice shattering, *J. Atmos. Oceanic Tech.*, *30*, 690–708, doi:10.1175/JTECH-D-12-00142.1.
Korolev, A. V., E. F. Emery, J. W. Strapp, S. G. Cover, and G. A. Isaac (2013a), Quantification of the effects of shattering on airborne ice particle measurements, *J. Atmos. Oceanic Tech.*, *30*, 2527–2553, doi:10.1175/JTECH-D-13-00115.1.
Korolev, A. V., et al. (2011), Small ice particles in tropospheric clouds: Fact or artifact? Airborne icing instrumentation evaluation experiment, *Bull. Am. Meteorol. Soc.*, *92*, 967–973, doi:10.1175/2010BAMS3141.1.
Krejci, R., J. Ström, M. Reus, and J. Williams (2005), Spatial and temporal distribution of atmospheric aerosols in the lowermost troposphere over the Amazonian tropical rainforest, *Atmos. Chem. Phys.*, *5*, 1527–1543, doi:10.5194/acp-5-1527-2005.
Kupiszewski, P., et al. (2015), The Ice Selective Inlet: A novel technique for exclusive extraction of pristine ice crystals in MPCs, *Atmos. Meas. Tech.*, *8*, 3087–3106, doi:10.5194/amt-83087-2015.

Lawson, R. P., L. J. Angus, and A. J. Heymsfield (1998), Cloud particle measurements in thunderstorm anvils and possible threat to aviation, *J. Aircr.*, *35*, 113–121, doi:10.2514/2.2268.
Lawson, R. P., D. O'Connor, P. Zmarzly, K. Weaver, B. Baker, Q. Mo, and H. Jonsson (2006), The 2D-S (stereo) probe: Design and preliminary tests of a new airborne, high-speed, high-resolution particle imaging probe, *J. Atmos. Oceanic Tech.*, *23*(11), 1462–1477, doi:10.1175/JTECH1927.1.
Lawson, R. P., S. Woods, and H. Morrison (2015), The microphysics of ice and precipitation development in tropical cumulus clouds, *J. Atmos. Sci.*, *72*(6), 2429–2445, doi:10.1175/Jas-D-14-0274.1.
Li, Z., F. Niu, J. Fan, Y. Liu, D. Rosenfeld, and Y. Ding (2011), Long-term impacts of aerosols on the vertical development of clouds and precipitation, *Nat. Geosci.*, *4*, 888–894, doi:10.1038/ngeo1313.
Liu, X., and J. E. Penner (2005), Ice nucleation parameterization for global models, *Meteor. Z.*, *14*, 499–514, doi:10.1127/0941-2948/2005/0059.
Lloyd, G., et al. (2015), The origins of ice crystals measured in mixed-phase clouds at the high-alpine site Jungfraujoch, *Atmos. Chem. Phys.*, *15*(22), 12,953–12,969, doi:10.5194/acp-15-12953-2015.
Lohmann, U., and J. Feichter (2005), Global indirect aerosol effects: A review, *Atmos. Chem. Phys.*, *5*, 715–737, doi:10.5194/acp-5-715-2005.
Lohmann, U., et al. (2007), Cloud microphysics and aerosol indirect effects in the global climate model ECHAM5-HAM, *Atmos. Chem. Phys.*, *7*, 3425–3446, doi:10.5194/acp-7-3425-2007.
Martin, G. M., D. W. Johnson, and A. Spice (1994), The measurement and parameterization of effective radius of droplets in warm stratocumulus clouds, *J. Atmos. Sci.*, *51*(13), 1823–1842, doi:10.1175/1520-0469(1994)051<1823:TMAPOE>2.0.CO;2.
Mertes, S., et al. (2007), Counterflow virtual impactor based collection of small ice particles in MPCs for the physico-chemical characterization of tropospheric ice nuclei: Sampler description and first case study, *Aerosol Sci. Technol.*, *41*, 848–864, doi:10.1080/02786820701501881.
Meyers, M. P., P. J. DeMott, and W. R. Cotton (1992), New primary ice-nucleation parameterizations in an explicit cloud model, *J. Appl. Meteorol.*, *31*, 708–721, doi:10.1175/1520-0450(1992)031<0708:NPINPI>2.0.CO;2.
Möhler, O., et al. (2003), Experimental investigation of homogeneous freezing of sulphuric acid particles in the aerosol chamber AIDA, *Atmos. Chem. Phys.*, *3*, 211–223, doi:10.5194/acp-3-211-2003.
Morrison, H., et al. (2009), Intercomparison of model simulations of mixed-phase clouds observed during the ARM Mixed-Phase Arctic Cloud Experiment. II: Multi-layered cloud, *Q. J. R. Meteorol. Soc.*, *135*, 1003–1019, doi:10.1002/qj.415.
Mossop, S. C. (1968), Comparison between concentration of ice crystals in cloud and the concentration of ice nuclei, *J. Rech. Atmos.*, *3*, 119–124.
Mossop, S. C. (1985), The origin and concentration of ice crystals in clouds, *Bull. Am. Meteorol. Soc.*, *66*(3), 264–273, doi:10.1175/1520-0477(1985)066<0264:TOACOI>2.0.CO;2.
Noone, K. J., et al. (1988), Design and calibration of a counterflow virtual impactor for sampling of atmospheric fog and cloud droplets, *Aerosol Sci. Tech.*, *8*, 235–244, doi:10.1080/02786828808959186.
Oraltay, R. G., and J. Hallett (1989), Evaporation and melting of ice crystals. A laboratory study, *Atmos. Res.*, *24*(1-4), 169–189.
O'Sullivan, D., et al. (2014), Ice nucleation by fertile soil dusts: Relative importance of mineral and biogenic components, *Atmos. Chem. Phys.*, *14*(4), 1853–1867, doi:10.5194/acp-14-1853-2014.
Petters, M., and T. Wright (2015), Revisiting ice nucleation from precipitation samples, *Geophys. Res. Lett.*, *42*, 8758–8766, doi:10.1002/2015GL065733.
Phillips, V. T. J., T. W. Choularton, A. J. Illingworth, R. J. Hogan, and P. R. Field (2003), Simulations of the glaciation of a frontal mixed-phase cloud with the Explicit Microphysics Model, *Q. J. R. Meteorol. Soc.*, *129*(590), 1351–1371, doi:10.1256/qj.02.100.
Phillips, V. T. J., P. J. DeMott, and C. Andronache (2008), An empirical parameterization of heterogeneous ice nucleation for multiple chemical species of aerosol, *J. Atmos. Sci.*, *65*, 2757–2783, doi:10.1175/2007JAS2546.1.
Pratt, K. A., et al. (2009), In situ detection of biological particles in cloud ice-crystals, *Nat. Geosci.*, *2*, 398–401, doi:10.1038/ngeo521.
Rosenfeld, D., and W. L. Woodley (2000), Deep convective clouds with sustained supercooled liquid water down to −37.5 C, *Nature*, *405*(6785), 440–442, doi:10.1038/35013030.
Rosenfeld, D., et al. (2014), Global observations of aerosol-cloud-precipitation-climate interactions, *Rev. Geophys.*, *52*, 750–808, doi:10.1002/2013RG000441.
Schwarzenboeck, A., F. Dezitter, A. Grandin, and A. Protat (2012), HighIWC—Ice water content of clouds at high altitude. EASA.2011.C30.
Seinfeld, J. H., et al. (2016), Improving our fundamental understanding of the role of aerosol−cloud interactions in the climate system, *Proc. Natl. Acad. Sci. U.S.A.*, *113*(21), 5781–5790, doi:10.1073/pnas.1514043113.
Stein, A. F., R. R. Draxler, G. D. Rolph, B. J. B. Stunder, M. D. Cohen, and F. Ngan (2015), NOAA's HYSPLIT atmospheric transport and dispersion modeling system, *Bull. Am. Meteorol. Soc.*, *96*, 2059–2077, doi:10.1175/BAMS-D-14-00110.
Strapp, W. et al., (2016), The high ice water content study of deep convective clouds: Report on science and technical plan. DOT/FAA/TC-14/31. [Available at http://www.tc.faa.gov/its/worldpac/techrpt/tc14-31.pdf.]
Tan, I., and T. Storelvmo (2016), Sensitivity study on the influence of cloud microphysical parameters on mixed-phase cloud thermodynamic phase partitioning in CAM5, *J. Atmos. Sci.*, *73*, 709–728, doi:10.1175/JAS-D-15-0152.1.
Taylor, J. W., et al. (2016), Observations of cloud microphysics and ice formation during COPE, *Atmos. Chem. Phys.*, *16*, 799–826, doi:10.5194/acp-16-799-2016.
Tobo, Y., et al. (2013), Biological aerosol particles as a key determinant of ice nuclei populations in a forest ecosystem, *J. Geophys. Res. Atmos.*, *118*, 10,100–10,110, doi:10.1002/jgrd.50801.
Twohy, C. H., and M. R. Poellot (2005), Chemical characteristics of ice residual nuclei in anvil cirrus clouds: Evidence for homogeneous and heterogeneous ice formation, *Atmos. Chem. Phys.*, *5*, 2289–2297, doi:10.5194/acp-5-2289-2005.
Twohy, C., et al. (2016), Abundance of fluorescent biological aerosol particles at temperatures conductive to the formation of mixed-phase clouds and cirrus clouds, *Atmos. Chem. Phys.*, *16*, 8205–8225, doi:10.5194/acp-16-8205-2016.
Vali, G. (1985), Nucleation terminology, *J. Aerosol Sci.*, *16*, 575–576.
Varble, A., et al. (2015), Evaluation of cloud-resolving and limited area model intercomparison simulations using TWP-ICE observations: 2. Precipitation microphysics, *J. Geophys. Res. Amos.*, *119*, 13,919–13,945, doi:10.1002/2013JD021372.
Vardiman, L. (1978), The generation of secondary ice particles in clouds by crystal–crystal collisions, *J. Atmos. Sci.*, *35*, 2168–2180.
Weber, R. J., A. D. Clarke, M. Litchy, J. Li, G. Kok, R. D. Schillawski, and P. H. McMurry (1998), Spurious aerosol measurements when sampling from aircraft in the vicinity of clouds, *J. Geophys. Res.*, *103*, 28,337–28,346, doi:10.1029/98JD02086.
Williams, E. R., R. Zhang, and J. Rydock (1991), Mixed-phase microphysics and cloud electrification, *J. Atmos. Sci.*, *48*(19), 2195–2203, doi:10.1175/1520-0469(1991)048<2195:MPMACE>2.0.CO;2.
Wilson, T. W., et al. (2015), A marine biogenic source of atmospheric ice-nucleating particles, *Nature*, *525*, 234–238, doi:10.1038/nature14986.
Zeng, X., et al. (2009), An indirect effect of ice nuclei on atmospheric radiation, *J. Atmos. Sci.*, *66*, 41–61, doi:10.1175/2008JAS2778.1.